RSC Advances

ROYAL SOCIETY OF CHEMISTRY

www.rsc.org/advances

Synthesis and Sub-10 nm Supramolecular Self-Assembly of a Nanohybrid with a Polynorbornene Main Chain and Side-Chain POSS Moieties

Ping-Ping Hou, Ke-Hua Gu, Yu-Feng Zhu, Zheng-Yu Zhang, Qian Wang, Hong-Bing Pan, Shuang Yang, Zhihao Shen,* and Xing-He Fan*

Beijing National Laboratory for Molecular Sciences, Key Laboratory of Polymer Chemistry and Physics of Ministry of Education, Center for Soft Matter Science and Engineering, College of Chemistry and Molecular Engineering, Peking University, Beijing, 100871, China

* To whom the correspondence should be addressed. E-mail: fanxh@pku.edu.cn (X.-H.F.); zshen@pku.edu.cn (Z.S.).

Abstract: A polynorbornene-based mesogen-jacketed liquid crystalline polymer (MJLCP) containing polyhedral oligomeric silsesquioxane (POSS) in the side chain, PNb10POSS, was synthesized through ring-opening metathesis polymerization. The chemical structure of the monomer was confirmed by $^{1}H/^{13}C$ NMR, high-resolution mass spectrometry, and elemental analysis. Molecular characterizations on the polymer were performed with ^{1}H NMR, gel permeation chromatography, and thermogravimetric analysis. The phase behavior of this new organic-inorganic hybrid polymer was investigated by differential scanning calorimetry,

polarized light microscopy, one-dimensional wide-angle X-ray scattering, synchrotron-radiation SAXS, two-dimensional wide-angle X-ray diffraction, and high-resolution transmission electron microscopy. With the competitive self-assemblies of the two covalently connected building blocks, namely MJLCP and POSS moieties, PNb10POSS shows various phase structures including an angstrom POSS crystal (Cr), a hexagonal columnar (Col_h) phase and the Cr coexisting, and the Col_h phase at different temperatures. The POSS crystal has a tremendous effect on the liquid crystalline (LC) behavior of the MJLCP. The results show that the competition between the crystallization of POSS and the LC formation of the polymer as a whole results in the complex phase behavior of the MJLCP-based nanohybrid. The polymer self-assembles into an organic-inorganic hybrid inclusion complex on the sub-10 nm scale. This work provides a new approach for the design and synthesis of ordered structures constructed by self-assembly on the sub-10 nm scale.

Keywords: Polyhedral oligomeric silsesquioxane (POSS), Ring-opening metathesis polymerization (ROMP), Self-assembly, Mesogen-jacketed liquid crystalline polymer (MJLCP), Inclusion complex

Introduction

Self-assembly on the nanometer scale is an interdisciplinary field connecting chemistry and many other subjects because it involves a wide range of aspects, such as design and synthesis of the building blocks in self-assembling systems, structures and functions of the self-assemblies,

supramolecular materials and devices, and so on. It can be divided into three major classes: (1) graft copolymer (polymer brush) self-assembly with sizes larger than 100 nm;[1, 2] (2) block copolymer self-assembly at 10–100 nm;[3, 4] (3) self-assembly with a size of about 10 nm or below (sub-10 nm).[5, 6] Recently ordered structures constructed by self-assembly on the sub-10 nm scale have attracted more and more attention.[7-10]

Generally, the building blocks in polymers that self-assemble on the sub-10 nm scale include one-dimensional (1D) rigid multi-benzene structures,[11] two-dimensional (2D) triphenylene structures[12] that act as mesogens, and three-dimensional (3D) fullerene (C60)[5, 13, 14] and polyhedral oligomeric silsesquioxane (POSS)[13, 15] that crystallize easily. Among these candidates, POSS has a precisely defined 3D molecular architecture and size, with the diameters of the inner and outer cages of about 0.45 and 1 nm,[15, 16] respectively. It has attracted many interests for its potential applications as engineering materials[15, 17] and fire-resistant materials.[15, 18]

Zhou et al.[19-21] have systematically studied mesogen-jacketed liquid crystalline polymers (MJLCPs), a special class of liquid crystalline (LC) polymers with stretched main chains due to the steric effect of the bulky side groups. MJLCPs self-assemble into ordered supramolecular structures, which can be columnar[12, 22] or smectic[23] LC phases. The LC properties are largely dependent on the chemical structures of the side groups, molecular weights (MWs) of the polymers, temperature, and so forth. In addition, MJLCPs can be excellent candidates to construct self-assemblies on the sub-10 nm scale. We have reported the self-assembled supramolecular structures of radically polymerized MJLCPs with 2D triphenylenes in the side

chains.[12, 24] The sub-10 nm scale nanostructures can be tuned by temperature and the length of the spacer in the side chain. Moreover, our recent work shows that a series of POSS-containing polymers with a polystyrene-based MJLCP main chain self-assemble into an organic-inorganic hybrid inclusion complex.[25] These polymers show various phase structures including sub-10 nm hexagonal columnar (Col_h) and columnar nematic LC phases, an angstrom rhombohedral crystalline (K_R) phase, and a hierarchically ordered phase with Col_h and K_R phases coexisting. However, vinyl monomers containing inorganic groups, especially C60, can hardly be polymerized through radical polymerization because of their ability to capture radicals. In addition, monomers with POSS can hardly be radically polymerized to afford polymers with high MWs owing to the bulkiness of POSS. And sometimes it is not easy to polymerize in solution because of the low concentration of vinyl groups in monomers. By changing the polymer main chain we may obtain inclusion complexes with different structures, length scales, and functionalities.

Olefin metathesis reaction has been applied to polymer science successfully, and a new polymerization method, ring-opening metathesis polymerization (ROMP),[26] has been developed. As a controllable polymerization method, ROMP has many advantages over radical or plasma polymerization. For example, by regulating the ratio of monomer to catalyst, the MWs of the polymers obtained can be controlled, and the polydispersity indexes (PDIs) can be quite low. Furthermore, polymers with high MWs can be obtained because the bulky pendants have little effect on the polymerization process. The most important point is that ROMP is tolerant to many functional groups, such as carbonyl, hydroxyl, ester, amide, halide, C60, etc.[26-29]

Recently we developed a new class of MJLCPs with polynorbornene main chains.[23] These new kind of polymers are easy to prepare and exhibit supramolecular self-assembled smectic A (SmA) phase for polymers with relatively long peripheral alkyl groups in the side chains. In this work, we designed and synthesized a new norbornene monomer containing crystalline POSS moieties. And the corresponding polymer was obtained by ROMP. The phase behavior and the supramolecular self-assembled structures at different temperatures were studied. We successfully obtained self-assembly on the sub-10 nm scale, confirming the rational design of the system.

Experimental Section

Materials and Characterization Methods. Dichloromethane (CH_2Cl_2) was treated by the Braun solvent purification system. *cis*-5-Norbornene-*exo*-2,3-dicarboxylic anhydride (96%) was purchased from J&K Chemical. (3-Hydroxypropyl)-heptaisobutyl-silsesquioxane (BPOSS-OH) was purchased from Hybrid Plastics. Tetrahydrofuran (THF, GPC) was distilled before use. Grubbs' catalyst (third generation) was purchased from Energy Chemical. All other reagents were obtained from commercial sources and used as received unless otherwise noted.

^{1}H NMR (400 MHz), ^{13}C NMR (100 MHz), high-resolution mass spectrometry (MS), elemental analysis (EA), one dimensional wide-angle X-ray scattering (1D WAXS), and 2D wide-angle X-ray diffraction (WAXD) experiments were performed according to the procedures reported.[12, 30] Thermogravimetric analysis (TGA) was conducted at a heating rate of 10 ^{o}C/min under a N_2 atmosphere. In differential scanning calorimetry (DSC) experiments, heating and cooling processes were conducted at rates of 20 and 5 ^{o}C/min, respectively, under a nitrogen

atmosphere. In polarized light microscopy (PLM) experiments, the sample was cast from a THF solution and slowly dried at ambient temperature. The polymer was first heated to 170 ^{o}C, followed by a cooling process and a second heating process. SAXS measurements in Shanghai synchrotron radiation facility were performed on the beamline BL16B1 using a three-slit system. The wavelength of the X-ray was 0.124 nm. The sample was mechanically sheared at 130 ^{o}C and then cooled to ambient temperature at a rate of 1 ^{o}C/min to ensure that the POSS moieties could crystallize and be tested in the heating process. In 2D WAXD experiments, the sample was treated the same way as for the sample for synchrotron-radiation SAXS measurements, but tested at ambient temperature. High-resolution transmission electron microscopy (HR-TEM) bright-field images were obtained with a Tecnai T20 TEM instrument using an accelerating voltage of 120 kV.

Synthetic Procedures.

The synthetic route is shown in Scheme 1. *N*-(2,5-Dicarboxylphenyl)-*cis*-5-norbornene-*exo*-2,3-dicarboximide (NbTA) was prepared as previously reported.[23]

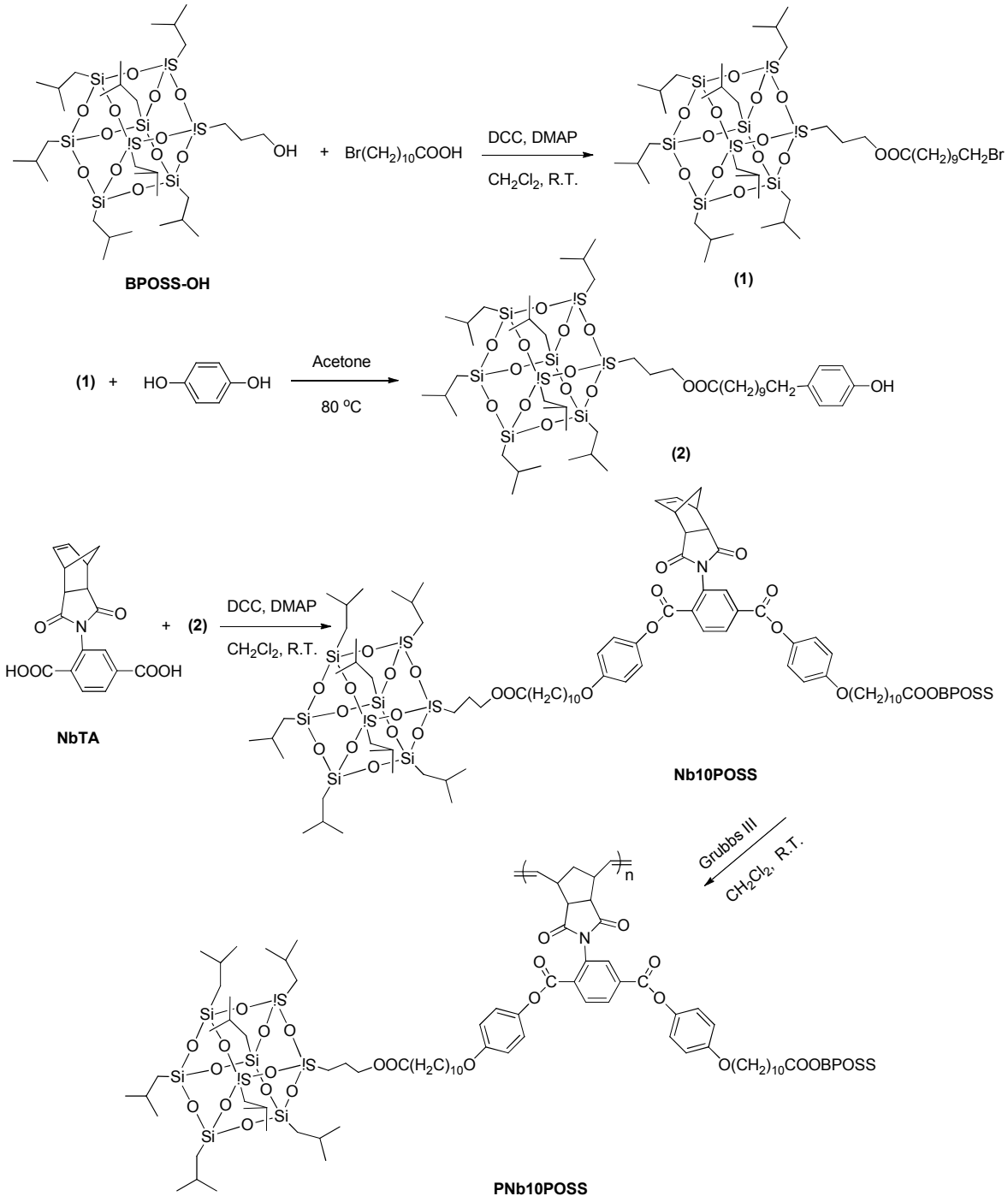

Scheme 1 Synthetic Procedure of PNb10POSS

Synthesis of Compound 1. BPOSS-OH (2.00 g, 2.25 mmol) and 50 mL of CH_2Cl_2 were charged in a 100 mL round-bottomed flask. 11-Bromoundecanoic acid (1.81 g, 6.79 mmol),

dicyclohexylcarbodiimide (DCC, 2.31 g, 11.2 mmol), and 4-dimethylaminopyridine (DMAP, 0.140 g, 1.23 mmol) were added to the flask. The mixture was stirred at ambient temperature for 24 h. Then the flask was cooled, and most DCC was removed by filtration. The liquid was condensed under a reduced pressure, and compound **1** was obtained by column chromatography as a white powder. Yield: 80%. ^{1}H NMR (400 MHz, $CDCl_3$, δ, ppm): 4.03 (t, 2H), 3.40 (t, 2H), 2.29 (t, 2H), 1.85 (m, 2H+9H), 1.71 (m, 2H), 1.62 (m, 2H), 1.29 (s, 12H), 0.96 (m, 42H), 0.61 (m, 16H). MS (HR-ESI): $[M + Na]^+/z$, Calcd. 1143.3458 g/mol; Found 1143.3488 g/mol. Anal. Calcd. C, 44.93; H, 7.99. Found: C, 44.93; H, 8.03.

Synthesis of Compound 2. Compound **1** (1.50 g, 1.32 mmol) was dissolved in 50 mL of acetone in a 100 mL round-bottomed flask. Then hydroquinone (1.45 g, 13.2 mmol) and K_2CO_3 (1.82 g, 13.2 mmol) were added to the flask. The mixture was refluxed at 80 ^{o}C for 18 h. Compound **2** was obtained as a white powder after column chromatography. Yield: 40%. ^{1}H NMR (400 MHz, $CDCl_3$, δ, ppm): 6.74 (m, 4H), 4.03 (t, 2H), 3.89 (t, 2H), 2.23 (t, 2H), 1.85 (m, 7H), 1.72 (m, 4H), 1.61 (m, 2H), 1.29 (m, 12H), 0.96 (m, 42H), 0.60 (m, 16H). MS (HR-ESI): $[M + H]^+/z$, Calcd. 1151.4774 g/mol; Found 1151.4756 g/mol. Anal. Calcd. C, 50.75; H, 8.34. Found: C, 50.68; H, 8.32.

The ^{1}H/^{13}C NMR spectra, mass spectroscopy results, and elemental analysis results of compounds **1** and **2** are shown in Supporting Information (Fig. S1−S8, Table S1).

Synthesis of the Monomer Nb10POSS**.** Compound **2** (0.601 g, 0.520 mmol), NbTA (0.0821 g, 0.250 mmol), and 20 mL of CH_2Cl_2 were added to a 50 mL round-bottomed flask. Then, DCC (0.440 g, 2.14 mmol) and DMAP (0.0261 g, 0.210 mmol) were added to the mixture.

The system was stirred at ambient temperature for 36 h. The product was obtained by column chromatography. After being recrystallized in methanol, the purified monomer was obtained as a white powder. Yield: 60%. ^{1}H NMR (400 MHz, $CDCl_3$, δ, ppm): 8.06□8.37 (m, 3H), 7.12 (m, 4H), 6.92 (m, 4H), 6.32 (s, 2H), 4.03 (t, 2H), 3.96 (m, 2H), 3.40 (s, 2H), 2.87 (s, 2H), 2.30 (t, 2H), 1.62□1.87 (m, 28H), 1.31 (m, 24H), 0.96 (d, 84H), 0.61 (s, 32H). ^{13}C NMR (100 MHz, $CDCl_3$, δ, ppm): 176.9, 173.9, 163.5, 157.2, 143.8, 143.5, 138.0, 130.8, 128.8, 122.2, 115.2, 68.4, 68.1, 66.2, 65.3, 48.5, 45.6, 43.5, 42.0, 38.7, 30.1, 29.7, 29.5, 29.4, 29.3, 29.2, 29.1, 28.9, 26.1, 25.7, 25.0, 23.9, 23.4, 23.1, 22.5, 22.4, 22.2, 14.1, 11.1, 8.4. MS (HR-ESI): $[M + H]^+/z$, Calcd. 2593.0002 g/mol; Found 2592.9978 g/mol. Anal. Calcd. C, 52.30; H, 7.65; N, 0.54. Found: C, 50.28; H, 7.67; N, 0.50.

Synthesis of PNb10POSS**.** Nb10POSS (70.0 mg, 26.7 μmol) and CH_2Cl_2 (0.15 mL) were charged into a dry Schlenk tube with a magnetic stir bar. After two freeze-pump-thaw cycles with high-purity nitrogen, third-generation Grubbs' catalyst (1.40 mg, 1.58 μmol) was added to the mixture. Then two freeze-pump-thaw cycles with high-purity nitrogen were conducted, followed by stirring at ambient temperature for 3 h. Vinyl ethyl ether (1 mL) was added to the mixture using a syringe, and the polymerization was stopped after an additional hour. The viscous liquid was diluted with 2 mL of CH_2Cl_2 and passed through a short alumina column to separate the catalyst. And then the polymer was precipitated out in 50 mL of methanol. After filtration and being dried in vacuum at 45 °C for 24 h, the target polymer PNb10POSS was obtained as a white solid. Yield: 57%.

Results and Discussion

Synthesis. The target monomer was obtained in four steps, and it was then polymerized through ROMP with the third-generation Grubbs' catalyst to yield the target polymer. Fig. 1 shows the ^{1}H NMR spectra of the monomer and the polymer in $CDCl_3$. The signal corresponding to hydrogens of the vinyl group in the monomer appears at 6.3 ppm. After polymerization, this resonance peak shifts to 5.5 ppm, and other peaks become broadened, suggesting the successful synthesis of the polymer PNb10POSS. The 100 MHz ^{13}C NMR spectrum of the monomer in $CDCl_3$ is given by Fig. S7 in Supporting Information. The GPC curve (Fig. 2) shows a unimodel and narrow distribution of molecular weights (MWs). The number-averaged MW (M_n) and the PDI value are 3.94×10^4 g/mol and 1.09, respectively.

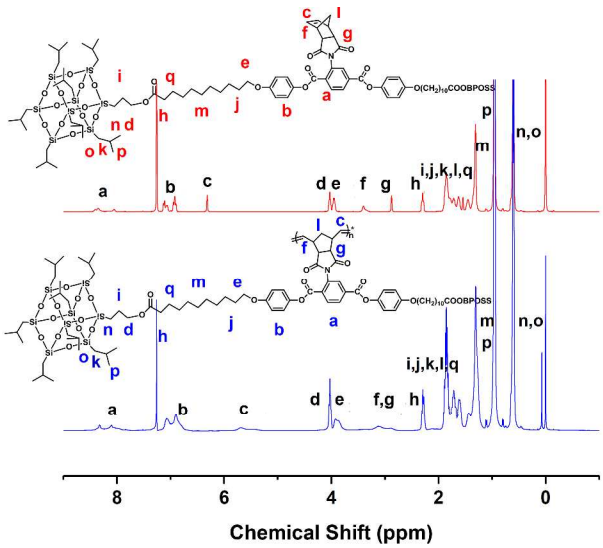

Fig. 1 400 MHz ^{1}H NMR spectra of Nb10POSS (top) and PNb10POSS (bottom) in $CDCl_3$.

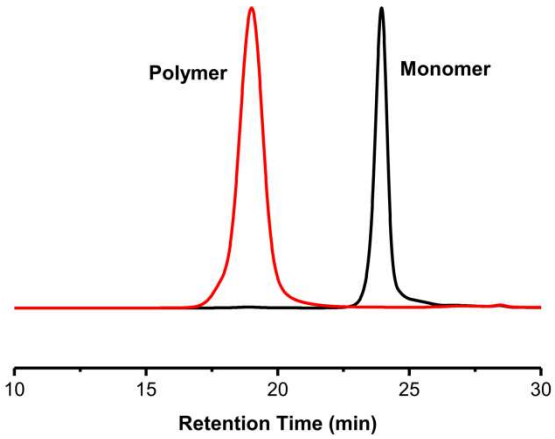

Fig. 2 GPC curves of Nb10POSS and PNb10POSS.

Thermal Properties of Polymer. As shown in Fig. S9 in Supporting Information, the 5% weight loss temperature of the polymer is 376 ^{o}C, indicating that the polymer exhibits an excellent thermal stability. Fig. 3 shows the first heating, first cooling, and second heating thermograms from DSC measurements. The first heating curve shows that the glass transition occurs at about 53 ^{o}C with a small change in heat flow, possibly due to the rigidity of the polymer chains leading to slow glass transition kinetics.[23] The endothermic peak at about 90 ^{o}C with an enthalpic change of 3.76 J/g (4.93 kJ/mol POSS) in the second heating process may be related to the melting of the POSS crystal. The peak at 150–170 ^{o}C with a smaller enthalpic change in heat flow during heating may correspond to the isotropization of PNb10POSS.

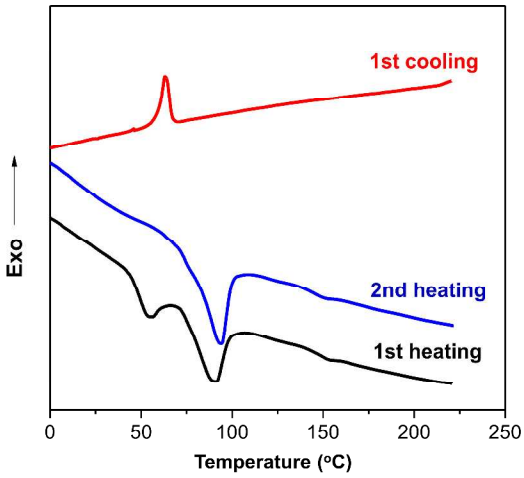

Fig. 3 DSC traces of the polymer in a nitrogen atmosphere.

Phase Structures of the Polymer. Phase behaviors were also examined by PLM, as shown in Fig. 4. The polymer shows strong birefringence at temperatures below 165 °C, which indicates a possible LC phase. Some of the micrographs at low temperatures show spherulite-like textures, possibly owing to the crystallized POSS moieties.

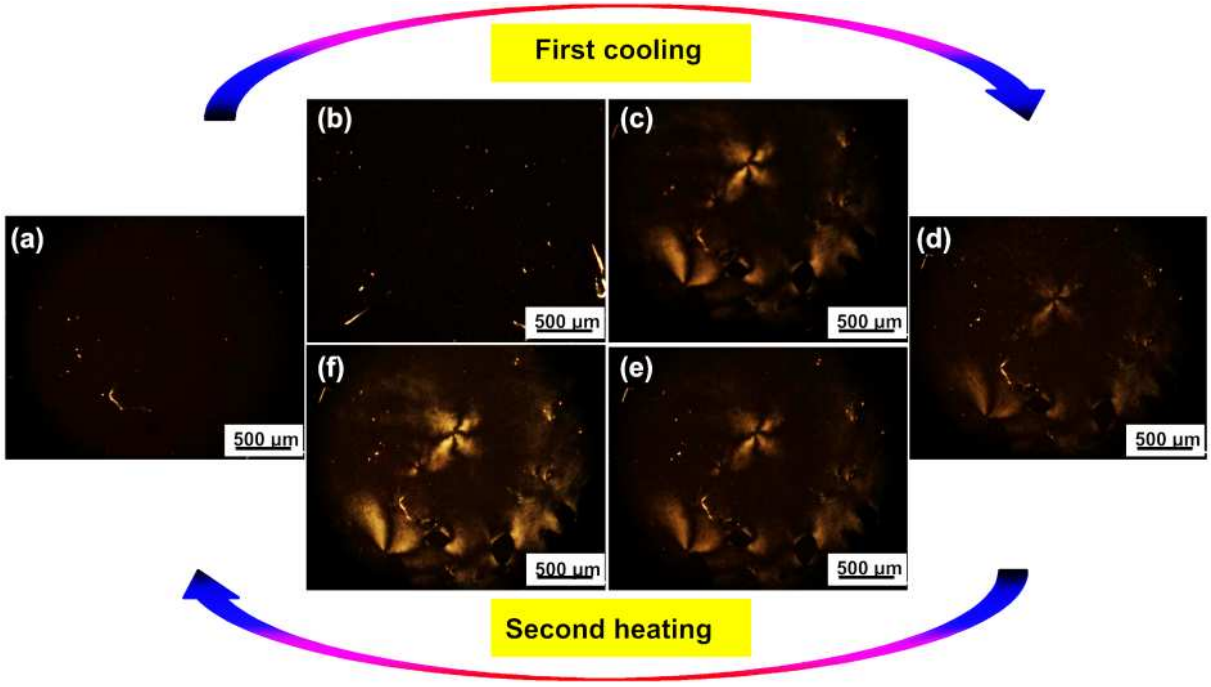

Fig. 4 PLM micrographs of the polymer at 165 (a), 140 (b), 130 (c) ^{o}C, and ambient temperature (d) during the first cooling process and those at 100 (e) and 150 (f) ^{o}C in the second heating process.

One-dimensional WAXS was used to investigate the phase structures of the polymer. As shown in Fig. 5a, at temperatures below 50 ^{o}C, there exist two peaks with q values of 5.84 and 7.79 nm^{-1} (corresponding d-spacing (d) values of 1.07 and 0.81 nm), respectively. These two peaks can be attributed to the crystalline structure (Cr) of POSS,[24] indicating that POSS moieties in the polymer form the crystalline structure in this temperature range. However, there is no peak in the even lower-angle region, indicating that the MJLCP-based polymer as a whole does not form an LC phase. When the temperature is above 50 ^{o}C, which is close to the glass transition temperature (T_g) of the polymer, a low-angle diffraction peak at q = 1.38 nm^{-1} appears, indicative of the development of the LC phase of the MJLCP due to the increased mobility of the polymer chains. The lack of a transition peak corresponding to the formation of the LC phase in the DSC heating curve is consistent with our previous reports of other MJLCPs that also do not show the LC formation in the DSC heating curves.[21, 31] When the temperature is increased to 100 ^{o}C, the intensity of the low-angle peak with q = 1.38 nm^{-1} increases, while the intensities of the two peaks originating from the POSS crystal decrease. This indicates that the LC phase becomes more ordered when the POSS crystal starts to melt. At 70 and 100 ^{o}C, both the diffraction peaks at q =1.38 and 5.84 nm^{-1} are sharp, suggesting the coexistence of the LC phase of the MJLCP and the Cr structure of POSS. At 150 ^{o}C, the diffraction peak at q = 5.84 nm^{-1} disappears, and a

scattering halo appears instead, while the diffraction peak at q = 1.38 nm^{-1} still remains. Such a result implies that the POSS crystal melts and the LC phase of the MJLCP retains. And at 170 ^{o}C, the low-angle diffraction peak also disappears, indicating that the MJLCP enters into the isotropic state. Therefore, the endothermic peaks ~150 ^{o}C with small enthalpic changes in DSC measurements during the heating processes correspond to the isotropization of the LC phase.

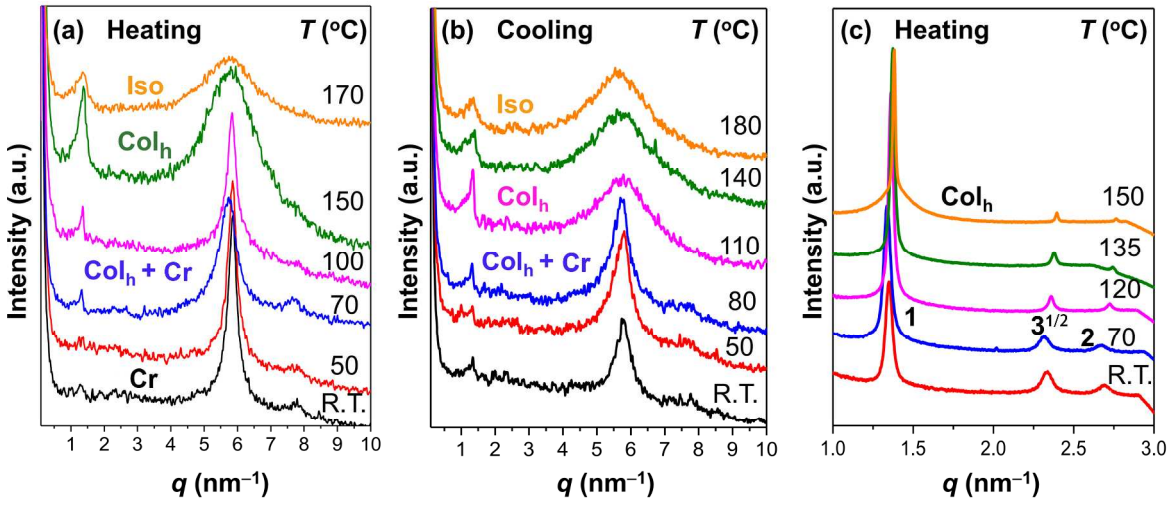

Fig. 5 1D WAXS profiles in the heating (a) and cooling (b) processes and synchrotron-radiation SAXS profiles in the heating process (c).

The transitions are mostly reversible during cooling, as shown in Fig. 5b. However, the LC phase of the MJLCP is retained at ambient temperature, as confirmed by the low-angle diffraction peak in the 1D WAXS profile. Such a phenomenon is quite common in many MJLCPs.[21, 31] The above results indicate that the structure of the polymer can be easily tuned by changing temperature.

However, the quality of the 1D WAXS data is not high enough to determine the structure of

the LC phase. Synchrotron-radiation SAXS was used to identify the LC structure. The results are shown in Fig. 5c. In the temperature range of 50 to 150 ^{o}C, there are three diffraction peaks in the low-angle region, and the scattering vector ratio is $1:3^{1/2}:2$. Taking the SAXS profile at 120 ^{o}C as an example, there exist three peaks at q =1.36, 2.37, and 2.74 nm^{-1} with a ratio of $1:3^{1/2}:2$. Thus, the LC phase of the polymer is a 2D Col_h structure with a lattice parameter a of 5.32 nm. The main chain and POSS moieties are chemically linked together with a relatively short spacer, of which the calculated length is ~1.26 nm with all methylene units adopting all-*trans* conformation.[25] With the addition of the sizes of POSS moieties and the rigid mesogenic core, the length of each side chain is about 6.0 nm. Therefore, the polymer main chains have to co-assemble with side-chain POSS moieties in the 3D space with each polymer chain acting as a supramolecular mesogenic unit. The diffraction peaks shift toward higher q values with increasing temperature, which should be owing to the relatively long alkyl chains adopting more and more gauche conformations.[32]

Fig. 6 illustrates the 2D WAXD result of the sheared polymer sample at ambient temperature. The X-ray beam was perpendicular to the shear direction. As shown in Fig. 6a, in the low-angle region, there are two pairs of diffraction arcs on the equator. And the integration of these two diffractions in Fig. 6c demonstrates that they have a scattering vector ratio of $1:3^{1/2}$. This result is consistent with synchrotron-radiation SAXS results and further confirms the Col_h LC structure of the MJLCP. The diffractions in the high-angle region are attributed to the Cr structure of the POSS crystal, indicating the coexistence of the Cr structure and the Col_h LC phase of the MJLCP.

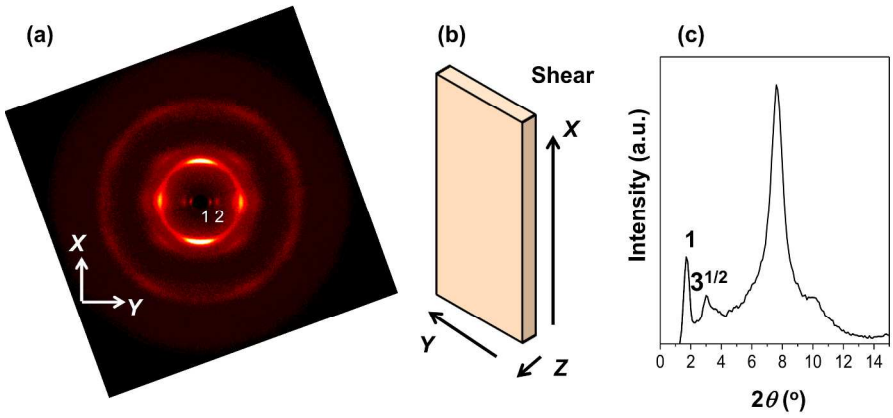

Fig. 6 2D WAXD pattern of the polymer at ambient temperature with the X-ray beam perpendicular to the shear direction (a), schematic drawing of the shearing geometry with the *X*-axis as the shear direction (b), and the integration curve (c) of (a).

As shown in Fig. 6a, diffractions 1 and 2 are (100) and (110) diffractions, respectively, of the Col_h structure on the sub-10 nanometer scale. The diffractions in the high-angle region are attributed to the crystal structure of the POSS moieties. However, the number of diffractions is not large enough to determine the exact structure of the POSS crystal and the relative orientation of the polymer main chain and the lattice of the POSS crystal. Because the diffractions could not be fitted into a K_R structure, the POSS moieties are likely packed in a triclinic crystalline structure (K_T) at the angstrom level with slight deviation from the K_T crystal of *iso*-butyl-POSS.[33]

We reconstructed the electron density map, as shown in Fig. 7, of the polymer from the synchrotron-radiation SAXS profile at 100 ^oC. The Col_h structure can be clearly observed. The distance between every two hexagons is about 5.2 nm, which is in good agreement with the value

calculated from the synchrotron-radiation SAXS data. Therefore, we assume that every hexagon represents a polymer chain. The red zone with the highest electron density, the blue zone with the lowest electron density, and the yellow and green zones in the middle with medium electron density should be POSS moieties, polynorbornene main chain, and flexible spacers, respectively.

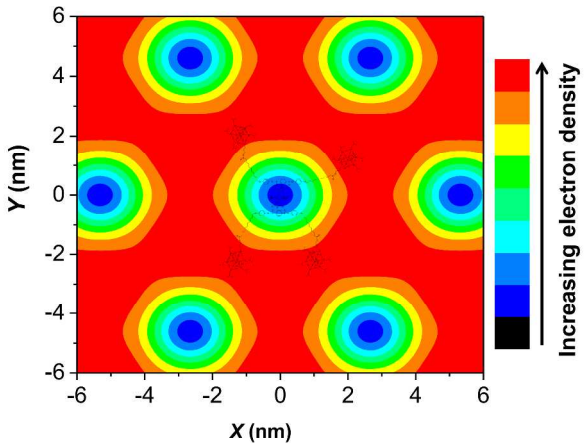

Fig. 7 Reconstructed electron density map of the polymer.

We also investigated the morphology of PNb10POSS with HR-TEM. A microtome-sliced thin film sample after 1D WAXS experiments was used. Striped structure is clearly observed in Fig. 8. The distance between neighboring strips is about 5.08 nm, which is in good agreement with the column-to-column distance (the value of the lattice parameter *a*, 5.32 nm) of the Col_h structure at ambient temperature calculated from the synchrotron-radiation SAXS profile in Fig. 5c.

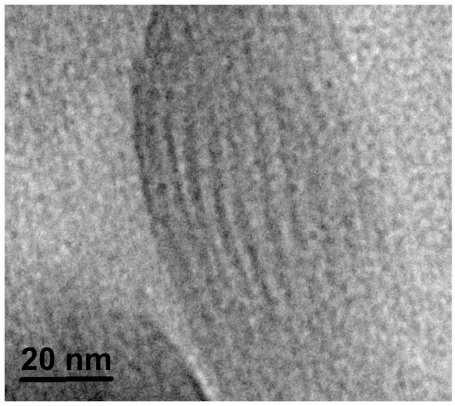

Fig. 8 HR-TEM micrograph of PNb10POSS.

On the basis of the above results, the phase diagram of the polymer can be illustrated in Fig. 9. At lower temperatures, the polymer exhibits the Cr structure of POSS coexisting with the Col_h LC phase of the MJLCP. At medium temperatures, the POSS crystal melts, and the MJLCP Col_h phase remains. At higher temperatures, the Col_h phase isotropilizes. Due to the slow kinetics and the disruption of the POSS crystal, the as-prepared polymer as a whole is not liquid crystalline, and the Col_h phase is formed when the chains are mobile enough during heating. Comparing with our very recent work,[25] again we successfully generated an organic-inorganic hybrid inclusion complex after changing the polystyrene main chain to a polynorbornene main chain. As expected, the length scale of the ordered structure increases from less than 5 nm to ~5.5 nm due to the larger dimension of the rigid part of the polymer chain.

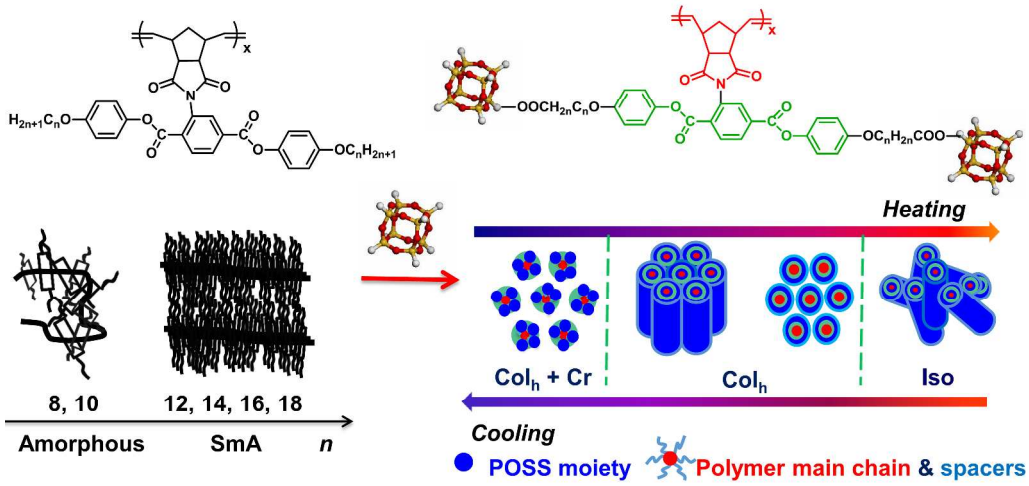

Fig. 9 Schematic drawing of the phase behaviors of polynorbornene-based MJLCPs PNbnPTs and PNb10POSS.

We have reported a new kind of MJLCPs (PNb*n*PTs) with polynorbornene main chains, where *n* is the number of carbon atoms in the alkyl tails in the side chain.[23] The LC properties of these polymers depend on the value of *n*. When *n* is 12, 14, 16, or 18, PNb*n*PT develops into the SmA phase. However, PNb*n*PTs are amorphous when *n* is 8 or 10. Therefore, we chose *n* = 10 in the hybrid polymer PNb10POSS in this work to study the influence of POSS on the phase behavior of the polymer. It has been reported that the melting temperatures of octaisobutyl POSS and POSS connected to polymethacrylic acid (PMA) are 261 ^{o}C[34] and 112 ^{o}C,[35] respectively. However, the melting temperature of the POSS crystal in PNb10POSS is 90 ^{o}C, lower than the values mentioned above. This is mainly due to the fact that the side chain containing the POSS moieties in PNb10POSS is covalently connected to the rigid polynorbornene main chain, which undoubtedly disrupts the packing of POSS. It is also interesting that the incorporation of POSS

induces the polymer to form the Col_h phase, rather than the amorphous state for PNb10PT or the SmA phase for PNb*n*PTs that are liquid crystalline. The enhanced propensity for the LC formation in this polymer with the incorporation of POSS can be mainly attributed to the increased steric effect which forces the main chain to be more extended. And the bulky 3D structure of POSS favors the rod-like shape of the polymer, leading to the formation of the Col_h phase. From simulation data, the sizes of the POSS molecule and each repeating unit are about 1.0 and 0.5 nm,[23, 36, 37] respectively. Therefore, the size of each POSS corresponds to that of two repeating units that have four POSS molecules. Due to the bulkiness of the POSS molecule, the four POSS units have to be surrounding the stretched polymer chain, leading to the cylindrical shape of the polymer and, therefore, the formation of the Col_h phase, rather than the SmA phase formed by PNb*n*PTs (*n* = 12, 14, 16, 18). Furthermore, from the densities of the POSS crystal (1.15 g/cm^3)[34] and the polymer main chain or the alkyl chains (~1.05 g/cm^3), the volume fraction of POSS is 64%, and it is likely for a microphase-separated system like the polymer in this study to form a cylinder structure.

Comparison of the Hierarchical Structures of Hybrid Polymers with Polynorbornene and Polystyrene Main Chains. As shown by the abovementioned results, the POSS-containing MJLCP with a polynorbornene main chain can form a hierarchical structure with a sub-10 nm Col_h phase and an angstrom Cr structure coexisting at low temperatures, and it displays a Col_h phase at relatively high temperatures. From a molecular point of view, compared to POSS-containing MJLCPs with a polystyrene backbone, the polynorbornene main chain of

PNb10POSS in this work has a repeating unit distance of ~0.5 nm and is a more rigid main chain than polystyrene with a repeating unit distance of ~0.25 nm because of the double bonds and five-membered rings in the backbone. Owing to its increased rigidity, the polynorbornene backbone is still an effective main chain for the construction of MJLCPs, even though the density of side chains in a polynorbornene-based MJLCP is only about one half of that in a polystyrene-based MJLCP. However, the increased rigidity of the polynorbornene main chain and a decreased POSS content make the packing of POSS moieties more complicated and breaks the symmetry of the POSS crystal, which is likely a K_T structure[33] in PNb10POSS rather than the rhombohedral crystal (K_R) in the polystyrene-based MJLCPs.[25] In addition, the increase in main-chain rigidity also results in the lower degree of order of the POSS crystal in PNb10POSS, as indicated by the fact that its transition temperature and the corresponding enthalpic change (90 ^oC, 4.93 kJ/mol POSS) are much lower than those for the POSS-containing MJLCP with a polystyrene main chain (156 ^oC, 17.7 kJ/mol POSS).[25] And the lower degree of order of the POSS crystal in the polymer in this work than that in the polystyrene analogue is probably also owing to the lower density of POSS moieties around the polymer main chains originating from the longer repeating unit of the polynorbornene chain. The increased main-chain rigidity and a lower POSS density are also the reasons for the POSS crystal to deviate from the K_R structure found in the polystyrene-based inclusion complex.[25] Finally, the whole MJLCP polymer chain of PNb10POSS is not as rigid as those of the POSS-containing MJLCPs with a polystyrene backbone due to the lower density of side chains and the weaker "jacketing" effect, which leads to a lower isotropization temperature for PNb10POSS that can go into the isotropic state during

the heating process. As a result, the POSS-containing MJLCP with a polynorbornene main chain PNb10POSS exhibits a hierarchical structure with the Col_h phase and the Cr structure of POSS coexisting at low temperatures, a simple Col_h phase at medium temperatures, and the isotropic state at high temperatures, although the as-prepared polymer only shows the Cr structure and the Col_h phase is formed after thermal treatment.

Conclusions

We synthesized a new hybrid MJLCP with POSS as the nano-building block in the side chain. At low temperatures, the formation of the Col_h phase of the polymer competes with the crystallization of POSS. In fact, the Cr structure of POSS disrupts, although does not destroy, the LC phase of the MJLCP. When the POSS crystal melts, the long-range ordered Col_h phase still remains, and it isotropilizes at even higher temperatures. The size of the Col_h structure is 5.0□6.0 nm, indicating that it is formed by the MJLCP polymer chain as a whole and that we have successfully obtained the sub-10 nm supramolecular self-assembled inclusion complex in this polymer. Such a sub-10 nm hybrid inclusion complex may have potential applications in constructing functional nanodevices.

ASSOCIATED CONTENTS

Supporting Information Available: $^{1}H/^{13}C$ NMR spectra, mass spectroscopy results, and elemental analysis results of compounds **1** and **2**; ^{13}C NMR spectra of Nb10POSS and PNb10POSS; TGA curve of PNb10POSS.

Acknowledgements

We acknowledge the support from the National Natural Science Foundation of China (Grants 21134001, 21374002, and 20990232). We also thank the Shanghai Synchrotron Radiation Facility for the assistance with the SAXS experiments.

References:

1. R. Ducker, A. Garcia, J. Zhang, T. Chen and S. Zauscher, *Soft Matter*, 2008, **4**, 1774-1786.
2. L. Fang, Y. Li, Z. Chen, W. Liu, J. Zhang, S. Xiang, H. Shen, Z. Li and B. Yang, *ACS Applied Materials & Interfaces*, 2014, **6**, 19951-19957.
3. F. Zhou, T. Ye, L. Shi, C. Xie, S. Chang, X. Fan and Z. Shen, *Macromolecules*, 2013, **46**, 8253-8263.
4. L.-Y. Shi, Z. Shen and X.-H. Fan, *Macromolecules*, 2011, **44**, 2900-2907.
5. X. Yu, W.-B. Zhang, K. Yue, X. Li, H. Liu, Y. Xin, C.-L. Wang, C. Wesdemiotis and S. Z. D. Cheng, *Journal of the American Chemical Society*, 2012, **134**, 7780-7787.
6. Y. S. Jung, J. B. Chang, E. Verploegen, K. K. Berggren and C. A. Ross, *Nano Letters*, 2010, **10**, 1000-1005.
7. T. Ichikawa, M. Yoshio, A. Hamasaki, J. Kagimoto, H. Ohno and T. Kato, *Journal of the American Chemical Society*, 2011, **133**, 2163-2169.
8. X. F. Yu, K. Yue, I. F. Hsieh, Y. W. Li, X. H. Dong, C. Liu, Y. Xin, H. F. Wang, A. C. Shi,

G. R. Newkome, R. M. Ho, E. Q. Chen, W. B. Zhang and S. Z. D. Cheng, *Proceedings of the National Academy of Sciences of the United States of America*, 2013, **110**, 10078-10083.

9. M. Huang, C.-H. Hsu, J. Wang, S. Mei, X. Dong, Y. Li, M. Li, H. Liu, W. Zhang, T. Aida, W.-B. Zhang, K. Yue and S. Z. D. Cheng, *Science*, 2015, **348**, 424-428.

10. H. Liu, C. H. Hsu, Z. Lin, W. Shan, J. Wang, J. Jiang, M. Huang, B. Lotz, X. Yu, W. B. Zhang, K. Yue and S. Z. Cheng, *Journal of the American Chemical Society*, 2014, **136**, 10691-10699.

11. Zhang, M. A. Horsch, M. H. Lamm and S. C. Glotzer, *Nano Letters*, 2003, **3**, 1341-1346.

12. Y.-F. Zhu, X.-L. Guan, Z. Shen, X.-H. Fan and Q.-F. Zhou, *Macromolecules*, 2012, **45**, 3346-3355.

13. W.-B. Zhang, X. Yu, C.-L. Wang, H.-J. Sun, I. F. Hsieh, Y. Li, X.-H. Dong, K. Yue, R. Van Horn and S. Z. D. Cheng, *Macromolecules*, 2014, **47**, 1221-1239.

14. T. Nakanishi, *Chemical Communications*, 2010, **46**, 3425-3436.

15. S.-W. Kuo and F.-C. Chang, *Progress in Polymer Science*, 2011, **36**, 1649-1696.

16. W. Zhang and A. H. E. Müller, *Progress in Polymer Science*, 2013, **38**, 1121-1162.

17. B. Li, Y. Zhang, S. Wang and J. Ji, *European Polymer Journal*, 2009, **45**, 2202-2210.

18. A. Fina, H. C. L. Abbenhuis, D. Tabuani and G. Camino, *Polymer Degradation and Stability*, 2006, **91**, 2275-2281.

19. Q. F. Zhou, H. M. Li and X. D. Feng, *Macromolecules*, 1987, **20**, 233-234.

20. Q. Zhou, X. Zhu and Z. Wen, *Macromolecules*, 1989, **22**, 491-493.

21. X. F. Chen, Z. Shen, X. H. Wan, X. H. Fan, E. Q. Chen, Y. Ma and Q. F. Zhou, *Chem Soc Rev*, 2010, **39**, 3072-3101.

22. Q.-K. Zhang, H.-J. Tian, C.-F. Li, Y.-F. Zhu, Y. Liang, Z. Shen and X.-H. Fan, *Polym. Chem.*, 2014, **5**, 4526.

23. Y.-F. Zhu, Z.-Y. Zhang, Q.-K. Zhang, P.-P. Hou, D.-Z. Hao, Y.-Y. Qiao, Z. Shen, X.-H. Fan and Q.-F. Zhou, *Macromolecules*, 2014, **47**, 2803-2810.

24. Y. F. Zhu, H. J. Tian, H. W. Wu, D. Z. Hao, Y. Zhou, Z. H. Shen, D. C. Zou, P. C. Sun, X. H. Fan and Q. F. Zhou, *J. Polym. Sci. Pol. Chem.*, 2014, **52**, 295-304.

25. Y.-F. Zhu, W. Liu, M.-Y. Zhang, Y. Zhou, Y.-D. Zhang, P.-P. Hou, Y. Pan, Z. Shen, X.-H. Fan and Q.-F. Zhou, *Macromolecules*, 2015, **48**, 2358-2366.

26. C. W. Bielawski and R. H. Grubbs, *Progress in Polymer Science*, 2007, **32**, 1-29.

27. K. Nomura and M. M. Abdellatif, *Polymer*, 2010, **51**, 1861-1881.

28. L. Ding, M. Xie, D. Yang and C. Song, *Macromolecules*, 2010, **43**, 10336-10342.

29. M. A. Tasdelen, M. U. Kahveci and Y. Yagci, *Progress in Polymer Science*, 2011, **36**, 455-567.

30. L. Zhang, S. Chen, H. Zhao, Z. Shen, X. Chen, X. Fan and Q. Zhou, *Macromolecules*, 2010, **43**, 6024-6032.

31. C. Ye, H.-L. Zhang, Y. Huang, E.-Q. Chen, Y. Lu, D. Shen, X.-H. Wan, Z. Shen, S. Z. D. Cheng and Q.-F. Zhou, *Macromolecules*, 2004, **37**, 7188-7196.

32. Z.-Q. Yu, J. W. Y. Lam, C.-Z. Zhu, E.-Q. Chen and B. Z. Tang, *Macromolecules*, 2013, **46**, 588-596.

33. A. R. Bassindale, Z. Liu, I. A. MacKinnon, P. G. Taylor, Y. Yang, M. E. Light, P. N. Horton and M. B. Hursthouse, *Dalton Transactions*, 2003, DOI: 10.1039/B302950F, 2945-2949.

34. E. T. Kopesky, T. S. Haddad, R. E. Cohen and G. H. McKinley, *Macromolecules*, 2004, **37**, 8992-9004.

35. Y. Ishida, T. Hirai, R. Goseki, M. Tokita, M.-A. Kakimoto and T. Hayakawa, *Journal of Polymer Science Part A: Polymer Chemistry*, 2011, **49**, 2653-2664.

36. H. Tu, X. Wan, Y. Liu, X. Chen, D. Zhang, Q.-F. Zhou, Z. Shen, J. J. Ge, S. Jin and S. Z. D. Cheng, *Macromolecules*, 2000, **33**, 6315-6320.

37. H.-C. Yang, S.-Y. Lin, H.-C. Yang, C.-L. Lin, L. Tsai, S.-L. Huang, I. W.-P. Chen, C.-h. Chen, B.-Y. Jin and T.-Y. Luh, *Angewandte Chemie International Edition*, 2006, **45**, 726-730.

TOC Graphic for

Synthesis and Sub-10 nm Supramolecular Self-Assembly of a Nanohybrid with a Polynorbornene Main Chain and Side-Chain POSS Moieties

Ping-Ping Hou, Ke-Hua Gu, Yu-Feng Zhu, Zheng-Yu Zhang, Qiang Wang, Hong-Bing Pan, Shuang Yang, Zhihao Shen,* and Xing-He Fan*

Beijing National Laboratory for Molecular Sciences, Key Laboratory of Polymer Chemistry and Physics of Ministry of Education, Center for Soft Matter Science and Engineering, College of Chemistry and Molecular Engineering, Peking University, Beijing, 100871, China